INL/JOU-24-81070-Revision-0

Multiscale Modeling of Silicon Carbide Cladding for Nuclear Applications: Thermal Performance Modeling

December 2024

Gyanender Singh, Jianguo Yu, Fei Xu, Tiankai Yao, Peng Xu

Changing the World's Energy Future

Idaho National Laboratory

INL is a U.S. Department of Energy National Laboratory operated by Battelle Energy Alliance, LLC

INL/JOU-24-81070-Revision-0

Multiscale Modeling of Silicon Carbide Cladding for Nuclear Applications: Thermal Performance Modeling

Gyanender Singh, Jianguo Yu, Fei Xu, Tiankai Yao, Peng Xu

December 2024

Idaho National Laboratory
Idaho Falls, Idaho 83415

http://www.inl.gov

Prepared for the
U.S. Department of Energy
Under DOE Idaho Operations Office
Contract DE-AC07-05ID14517

energies

MDPI

Article

Multiscale Modeling of Silicon Carbide Cladding for Nuclear Applications: Thermal Performance Modeling

Gyanender Singh, Jianguo Yu, Fei Xu, Tiankai Yao and Peng Xu *

Idaho National Laboratory, Idaho Falls, ID 83415, USA; gyanender.singh@inl.gov (G.S.); jianguo.yu@inl.gov (J.Y.); fei.xu@inl.gov (F.X.); tiankai.yao@inl.gov (T.Y.)
* Correspondence: peng.xu@inl.gov

Abstract: The complex multiscale and anisotropic nature of silicon carbide (SiC) ceramic matrix composite (CMC) makes it difficult to accurately model its performance in nuclear applications. The existing models for nuclear grade composite SiC do not account for the microstructural features and how these features can affect the thermal and structural behavior of the cladding and its anisotropic properties. In addition to the microstructural features, the properties of individual constituents of the composites and fiber tow architecture determine the bulk properties. Models for determining the relationship between the individual constituents' properties and the bulk properties of SiC composites for nuclear applications are absent, although empirical relationships exist in the literature. Here, a hierarchical multiscale modeling approach was presented to address this challenge. This modular approach addressed this difficulty by dividing the various aspects of the composite material into separate models at different length scales, with the evaluated property from the lower-length-scale model serving as an input to the higher-length-scale model. The multiscale model considered the properties of various individual constituents of the composite material (fiber, matrix, and interphase), the porosity in the matrix, the fiber volume fraction, the composite architecture, the tow thickness, etc. By considering inhomogeneous and anisotropic contributions intrinsically, our bottom-up multiscale modeling strategy is naturally physics-informed, bridging constitutive law from micromechanics to meso-mechanics and structural mechanics. The effects that these various physical attributes and thermo-physical properties have on the composite's bulk thermal properties were easily evaluated and demonstrated through the various analyses presented herein. Since silicon carbide fiber-reinforced SiC CMCs are also promising thermal–structural materials with a broad range of high-end technology applications beyond nuclear applications, we envision that the multiscale modeling method we present here may prove helpful in future efforts to develop and construct reinforced CMCs and other advanced composite nuclear materials, such as MAX phase materials, that can service under harsh environments of ultrahigh temperatures, oxidation, corrosion, and/or irradiation.

Keywords: silicon carbide (SiC); multiscale modeling; cladding; nuclear; finite element; inhomogeneous; anisotropic

Citation: Singh, G.; Yu, J.; Xu, F.; Yao, T.; Xu, P. Multiscale Modeling of Silicon Carbide Cladding for Nuclear Applications: Thermal Performance Modeling. *Energies* **2024**, *17*, 6124. https://doi.org/10.3390/en17236124

Academic Editors: Guglielmo Lomonaco, Álvaro Rodríguez-Prieto and Fabio Panza

Received: 7 October 2024
Revised: 26 November 2024
Accepted: 28 November 2024
Published: 5 December 2024

1. Introduction

Silicon carbide (SiC) fiber-reinforced SiC matrix composite (SiC/SiC) is a candidate material for many nuclear applications in both fusion and fission reactors as fuel cladding and radiation blankets [1], as well as harsh, high-temperature structural applications, such as hot components in gas turbine engines, heat exchangers, reformers, reactors, and filters for the chemical industry. SiC/SiC exhibits exceptionally high temperature resistance [2], good irradiation stability [3], low neutron absorption [4], reasonable fracture toughness [5,6], and high corrosion resistance [7,8]. Comprehensive discussions on the properties of SiC/SiC composites are found in previous works [9,10]. Thanks to their favorable characteristics, SiC/SiC composites are being considered for use as fuel cladding and channel box materials in light water reactors [11,12] and for fuel and in-vessel components in high-temperature

gas-cooled reactors [13,14], fluoride-salt-cooled high-temperature reactors [15], sodium fast reactors [16], and for structural and functional components (e.g., flow channel inserts, pipes, and ducts in divertors) used in fusion reactor applications [17]. There are other candidate materials for accident tolerant fuel cladding applications such as coated and improved Zr alloy cladding and FeCrAl alloy cladding. The over-reliance of the coated Zr cladding on the physical integrity of its coating for its accident tolerance ability and increased neutron absorption of the FeCrAl cladding are the major technical concerns of these respective cladding concepts. Note that MAX phase materials have also been identified as potential materials for use in current and future reactor systems due to their unique combination of properties, including high thermal conductivity, mechanical strength, damage tolerance, and resistance to thermal shock. However, SiC/SiC generally offers superior high-temperature resistance and radiation tolerance, making them potential materials as nuclear fuel cladding. In contrast, MAX phases stand out due to their ease of machinability and thermal conductivity, making them more suitable for components requiring complex shapes, and high thermal stress resistance within a reactor system.

The qualification process requires a better understanding of the material's performance—as well as that of components made from this material—within the intended environment. Thermal–mechanical computational analysis provides insights into the stresses and temperature distributions pertaining to a given component, as well as its structural integrity and thermal performance under different operating scenarios and accident conditions. Most computational studies conducted on SiC cladding to determine the engineering-scale thermal–mechanical performance of SiC/SiC have assumed a homogenized material, neither resolving the fibers, matrix, interphase, or porous voids nor accounting for the specific architecture of the composite [18–24]. By focusing only on the composite's bulk properties, this approach may work for a particular composite with fixed architecture, porosity, fiber volume fraction, etc. However, such analysis is unable to elucidate how the micro-level thermo-physical properties and architecture impact the performance of a component made of composite material. Few studies have investigated the microstructure and architecture of composites in fusion and non-nuclear applications. Nevertheless, historically speaking, analyses of composites are difficult because of the complex multiscale and anisotropic nature of the SiC/SiC composite material itself.

A composite consists of a stack of plies (also called as laminate) each comprising tows of fibers coated with interphase material and embedded inside a matrix material. The composite can feature unidirectional, bidirectional (woven), multidirectional (quasi-isotropic), or randomly oriented fibers. Depending on the intended application, the fibers can be continuous or short in length and may be woven, braided, or knitted. The order and orientation of the plies in the laminate are carefully selected to impart the desired directional and structural properties. To prevent delamination, interlaminar reinforcement is sometimes added through techniques such as stitching or z-pinning. During the manufacturing process, pockets of air may remain trapped within the composite material, leading to a porous structure with voids. These voids may significantly affect the performance of the composite.

A model for predicting the performance of a composite must account for the effects of fiber spacing, fiber volume fraction, orientation, porosity (pore size/distribution), the mechanical properties of the fibers and the matrix, architecture, orientation of the material (with respect to the component's geometric direction, e.g., axis), tow thickness, number of plies, etc. Accounting for these and other geometric variables, as well as any physical and material property variations, makes such models computationally very expensive. Furthermore, interactions among the constituents add complexity to the involved physics, in turn making it challenging to solve numerically, resulting in numerous challenges in modeling and analyzing composites.

Many different approaches to modeling composites are found in the literature. Under the umbrella of micromechanical modeling, there are methods such as analyzing a representative volume element to obtain the effective properties of the composite; using a rule of

mixtures to estimate the weighted average of properties based on the volume fraction of the constituents; and using analytical homogenization techniques to calculate the effective properties in consideration of the interaction occurring between different phases. Theoretical methods such as classical laminate theory, first-ply failure analysis, and shear-lag modeling all fall into the category of micromechanical modeling and analysis. These theoretical models are useful when detailed microstructure is not the primary concern. Thus, these models are unable to describe the microstructural features and how these features can affect the thermal and structural behavior of the cladding and the anisotropic properties. There are also several multiscale modeling methods, such as hierarchical multiscale modeling, concurrent multiscale modeling, and representative volume element coupling. These are useful when local microstructural effects such as damage initiation and propagation are considered important. However, these models for determining the relationship between the individual constituents' properties and the bulk properties of the composite are absent, although empirical relationships exist in the literature.

In the present work, we utilized a hierarchical multiscale modeling approach to model SiC/SiC composites in a modular manner. This approach essentially entails breaking down the complexity of a composite material into simpler models at different length scales and allowing the complexity to be incorporated into the model. Though in this work we aimed to model SiC/SiC fuel cladding for nuclear applications, the same approach is generally applicable to composites used for all types of applications.

2. Methods

The hierarchical multiscale modeling approach involved several models operating at different length scales. Starting with the micro-level model, the bulk properties were computed based on the properties of the constituents. These evaluated bulk properties were then utilized as an input to the model at a higher length scale. In this manner, the engineering-scale properties were calculated in consideration of the effects of the individual constituent's properties (fibers, matrix, and interphase), physical features (e.g., microcracks, pores), and architectural parameters (e.g., fiber volume fraction, relative tow orientation, fiber density in tows, etc.). Note that the hierarchical multiscale modeling involved the sequential calculation of the properties at each length scale. This approach differed from the concurrent multiscale modeling approach in which calculations at different length scales were performed simultaneously, thus requiring significant computational resources.

Figure 1 illustrates the hierarchical multiscale modeling. In the present work, we considered models pertaining to four length scales: (1) tow and matrix models, (2) a ply model, (3) a laminate model, and (4) a component (cladding) model. In the tow model, fibers were embedded in a matrix and were potentially surrounded by pores. Please note that for simplicity, the interphase was not considered in the current model but will be incorporated into future work. Currently, the most commonly used layered interphase for nuclear applications is pyrolytic carbon (PyC). The thermal conductivity of PyC is slightly lower than that of the fiber; however, the thickness of the PyC coating is much smaller than the fiber diameter. Thus, it was expected that the presence of the interphase would have a small influence on the general thermal behavior. A detailed analysis incorporating the interphase in the fiber will be performed in future work to fully understand these effects.

The ply-level model featured tows arranged together in a particular architecture with a matrix surrounding the fiber. For this model, the matrix properties were obtained from a matrix model in which pores were impregnated into the matrix material. The laminate model was comprised of two or more plies stacked together, each with a particular orientation relative to the others. Finally, at the highest scale, there was the cladding model containing the desired geometric parameters (e.g., radius, thickness, and length). The CAD version of these models was generated either through the Cubit software (version 15.2) [25] or SolidWorks™ software (version 2023) from Dassault Systèmes or through the Multiphysics Object-Oriented Simulation Environment (MOOSE) [26] internal mesh generators. The models generated using Cubit and SolidWorks™ software were meshed

using the Cubit software with the tetrahedral elements. The models generated by MOOSE were automatically meshed within the MOOSE. The meshes were refined enough to obtain a converged solution.

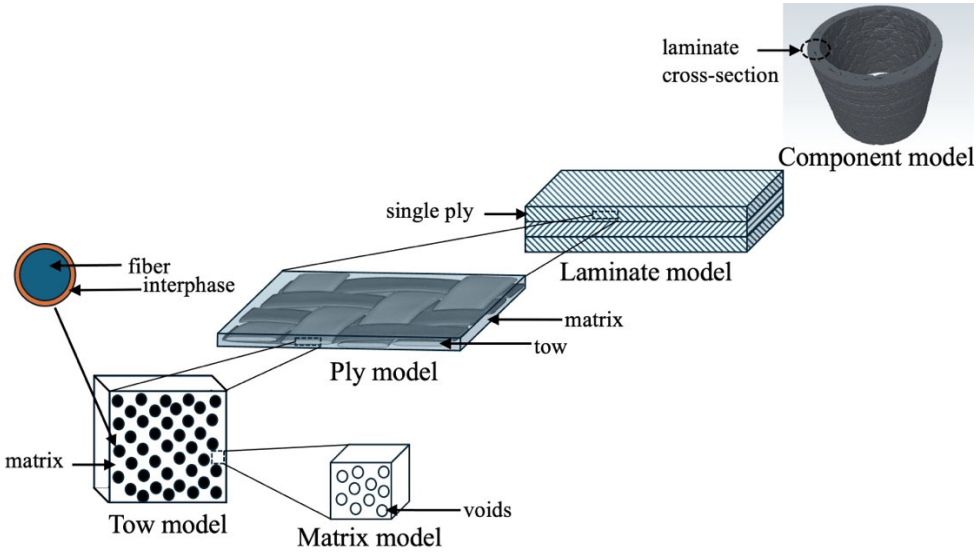

Figure 1. Hierarchical multiscale modeling approach for modeling SiC cladding.

In each of the models, the thermal properties of the constituents were taken as the input. Specifically, the output of the thermal conductivity from the matrix model was the input for the thermal conductivity of the matrix in the tow model; the output of the thermal conductivity of the tow model was the input for the thermal conductivity of the tow in ply model; the output of the thermal conductivity from the ply model was the input for the thermal conductivity of the ply in the laminate model; and the output of the thermal conductivity of the laminate model served as the input for the thermal conductivity of the component (cladding) model. Figure 2 shows how the thermal conductivity was calculated via the numerical analysis of the model. In this analysis, heat flux (q'') and temperature (T) boundary conditions were prescribed on two opposite faces of the model, in addition to the thermal properties of the model constituents. Thermal analysis was performed to obtain the temperature distribution in this model. The bulk thermal conductivity of the model was obtained per Equation (1), using the calculated temperature, where ΔT denoted the temperature gradient along the direction perpendicular to the two faces. All thermal calculations were performed with the MOOSE.

$$k = -\frac{q''}{\Delta T} = \frac{q'' L}{T_1 - T_2} \quad (1)$$

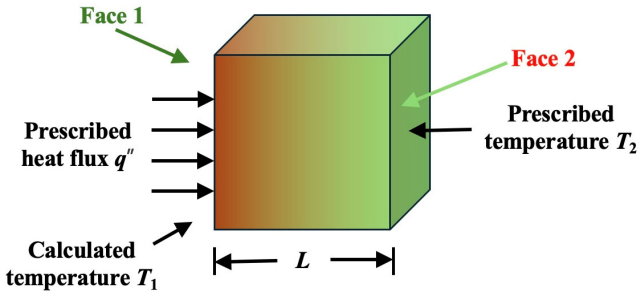

Figure 2. Schematic showing how thermal conductivity (k) was calculated via numerical analysis. Fourier's law was used to evaluate the bulk thermal conductivity of the model.

3. Results

In this section, we demonstrated the functionality of this model by using numerical calculations to obtain the properties at the highest scale based on the properties of each constituent at the microstructural scale.

Matrix model: The matrix model represented the matrix material containing the pores and voids that could develop throughout the manufacturing process. In the model, the voids were represented as spherical cavities, as shown in Figure 3. The same figure also shows a mesh of the model, and an example temperature distribution obtained from an analysis for computing the bulk thermal conductivity. The thermal properties of the pores and voids handled in the model are assumed to be vacuum. Figure 4 shows the variation in the matrix thermal conductivity with the change in porosity.

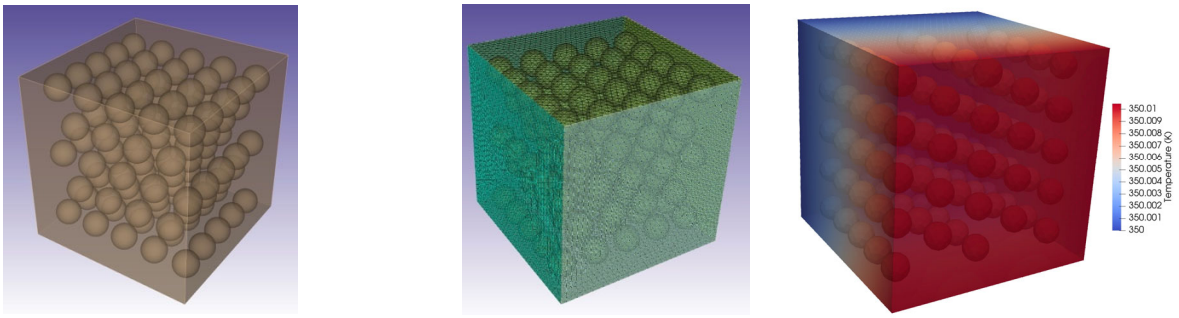

Figure 3. (**Left**) Computer-aided design (CAD) model of the matrix. (**Middle**) Mesh of the model. (**Right**) An example temperature distribution obtained through an analysis.

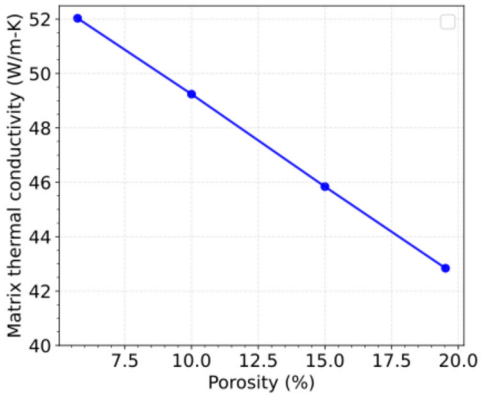

Figure 4. Variation in matrix thermal conductivity with porosity as obtained from the matrix model.

Tow model: The tow model represented a tow whose constituent fibers were all lying in one direction. The fiber orientation gives a tow its anisotropic properties. Figure 5 shows a computer-aided design (CAD) image and mesh of a tow model. Figure 6 shows, for a particular set of constituent thermal properties, the temperature distributions for the two cases considered: (a) heat flow along the fiber direction and (b) heat flow perpendicular to the fiber direction. Case (a) was considered for obtaining the tow's bulk thermal conductivity along the direction of the fibers, and case (b) provided the tow's bulk thermal conductivity in the direction perpendicular to the fibers.

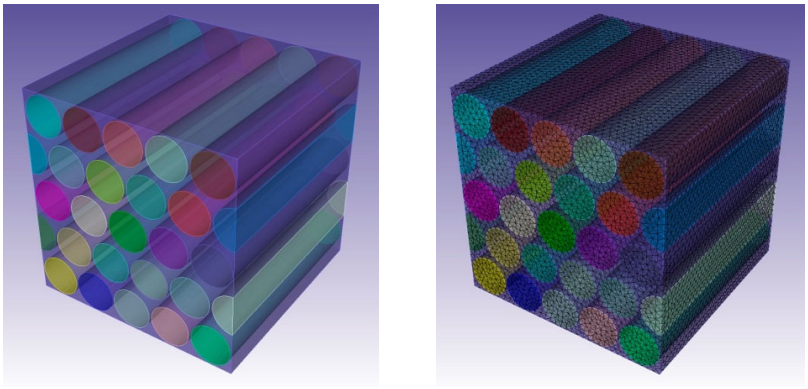

Figure 5. (**Left**) CAD model of a tow. (**Right**) Mesh of the model.

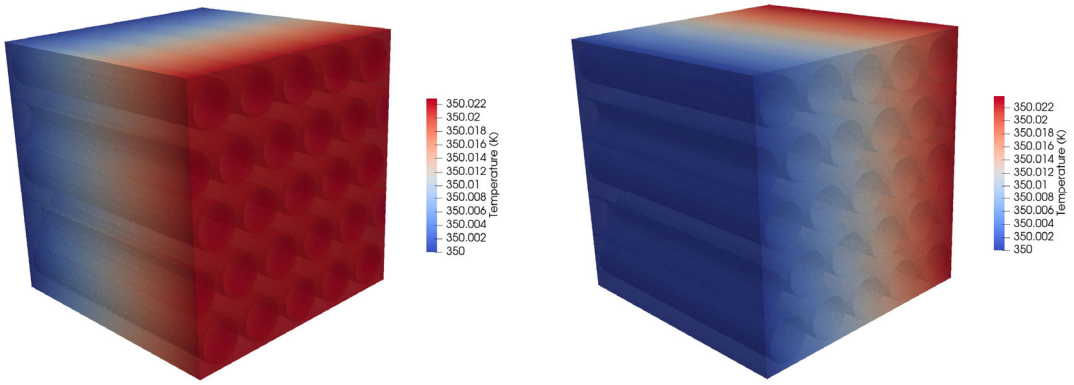

Figure 6. Temperature distribution in the tow model for two separate cases: heat flow along the fiber direction (**left**) and heat flow perpendicular to the fiber direction (**right**).

As described in the Methods Section and illustrated in Figure 2, the thermal properties of the fibers and matrix were added to the model. Our assumption in this analysis was that the fibers and matrix had isotropic properties. Figure 7 shows the varying tow thermal conductivity in response to changes in the thermal conductivities of the fibers and matrix in which the volume fraction of the fiber used was 69.4%. This model considered different levels of fiber volume fraction in the tow region (see Figure 8), as well as how changes to the fiber volume fraction impacted the tow's thermal conductivity (see Figure 9). As noted from the tow model, inhomogeneous and anisotropic characterizations were considered naturally and intrinsically.

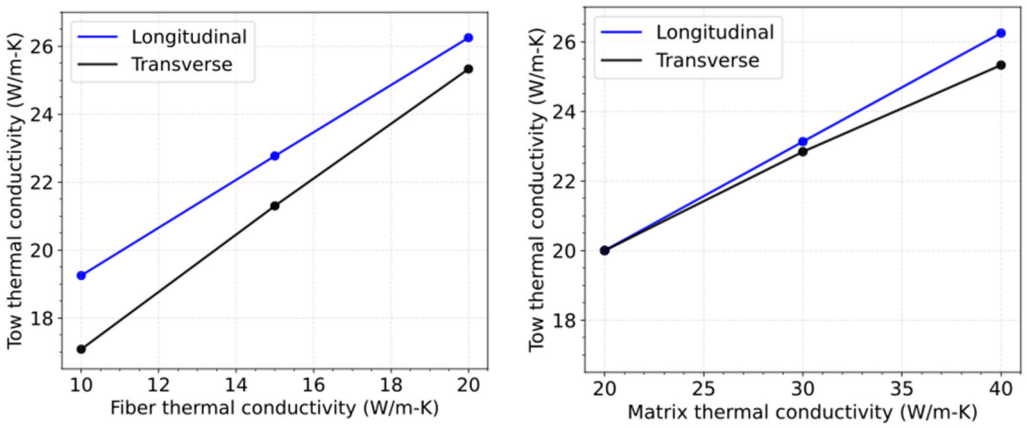

Figure 7. Variation in a tow's bulk thermal conductivity when varying the thermal conductivity of the fibers (**left**) (k_{matrix} = 40 W/m-K) and matrix (**right**) (k_{fiber} = 20 W/m-K).

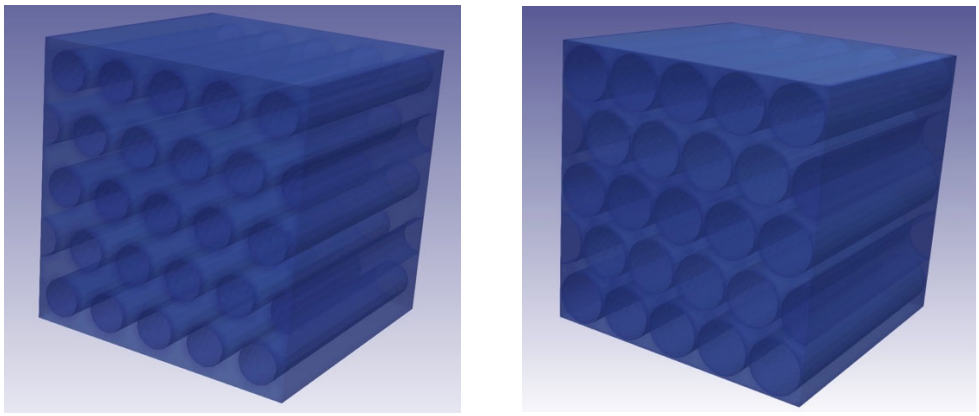

Figure 8. Tow models with fiber volume fractions of 38.5% (**left**) and 69.4% (**right**).

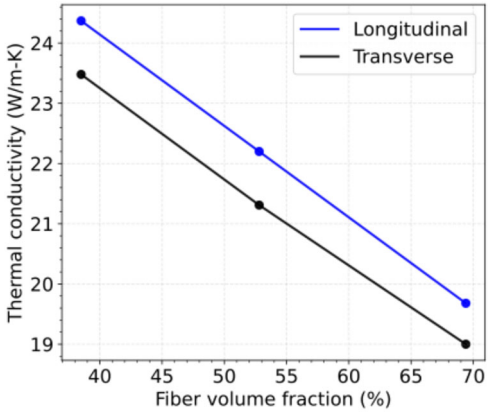

Figure 9. Variation in the tow's bulk thermal conductivity in response to changing the volume fraction of the fibers (k_{matrix} = 30 W/m-K) and the matrix (k_{fiber} = 15 W/m-K).

Ply model: SiC cladding plies (or lamina) consisted of tows weaved together. Figure 10 shows a CAD model of a single volume element of a ply, along with a single tow. The meshes are shown in Figure 11. As seen from these figures, the ply's anisotropic properties stemmed from the orientation of the tows; the in-plane properties differed from those in the through-thickness direction. Figure 12 shows the temperature distributions in the ply model for the two cases considered here: (a) heat flow along the plane of the ply and (b) heat flow perpendicular to the ply. Case (a) was considered for evaluating the ply's bulk thermal conductivity along the plane of the ply, and case (b) provided its bulk thermal conductivity in the direction perpendicular to the plane of the ply. The thermal properties of the tows and matrix were inputted into the model. It was assumed that the matrix had isotropic properties and that the tows had anisotropic properties stemming from the fiber orientation (as noted earlier). Figure 13 shows the variation in the ply's bulk thermal conductivity in response to varying the thermal conductivities of the tows and matrix. By considering inhomogeneous and anisotropic characterizations intrinsically at the tow level, the anisotropic feature was naturally found at the ply level via our bottom-up multiscale modeling strategy.

Equation (2) shows the form of Fourier's law for the anisotropic heat conduction. The subscript "*long*" refers to the longitudinal direction, "*trans*" refers to the transverse direction (see Figure 10), and "*l*" refers to the coordinate distance.

$$\begin{bmatrix} q''_{long} \\ q''_{trans1} \\ q''_{trans2} \end{bmatrix} = - \begin{bmatrix} k_{long} & 0 & 0 \\ 0 & k_{trans1} & 0 \\ 0 & 0 & k_{trans2} \end{bmatrix} \begin{bmatrix} dT/dl_{long} \\ dT/dl_{trans1} \\ dT/dl_{trans2} \end{bmatrix} \quad (2)$$

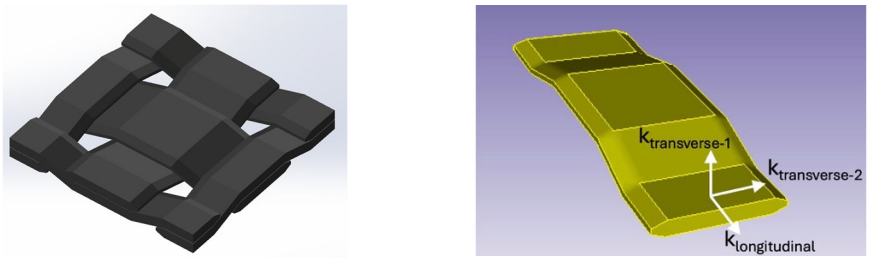

Figure 10. (**Left**) CAD model of a single volume element of weaved tows in a ply. (**Right**) A single tow. The computational framework allows for considering tows' anisotropic properties, which stem from fiber orientation, providing the different longitudinal ($k_{longitudinal}$) and transverse thermal conductivities ($k_{transverse}$) in a tow.

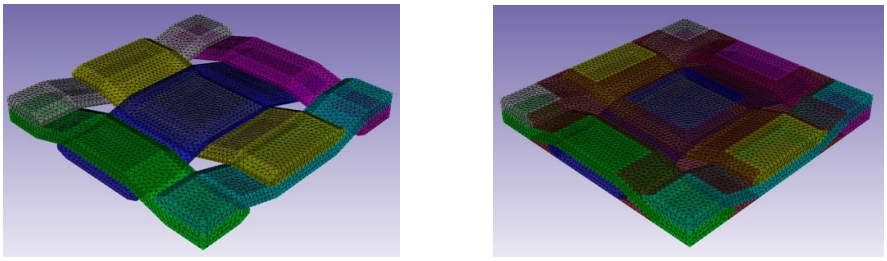

Figure 11. Mesh single volume element of weaved tows (**left**) surrounded by a meshed matrix (**right**).

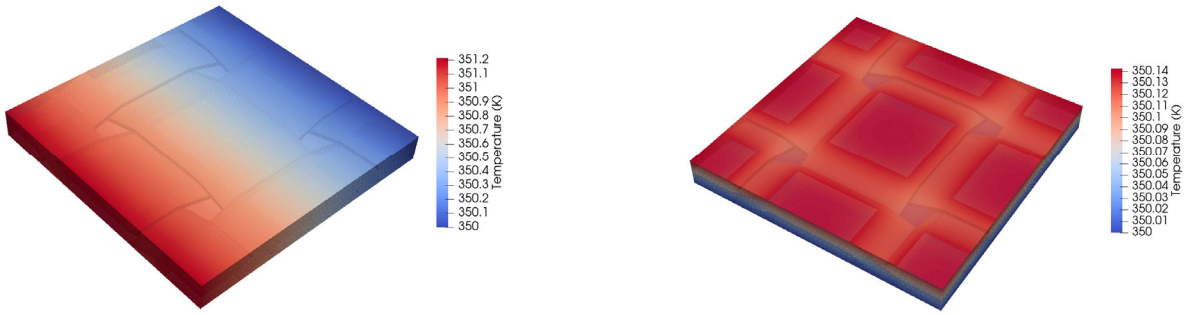

Figure 12. Temperature distribution in the ply model for the two selected cases: heat flow along the plane of the ply (**left**) and heat flow perpendicular to the plane of the ply (**right**).

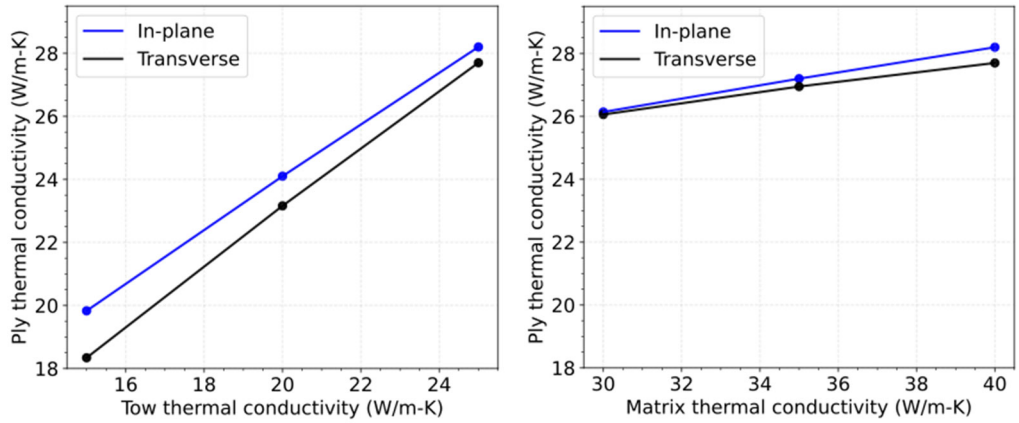

Figure 13. Variation in ply thermal conductivity in response to varying the tow thermal conductivity (**left**) and matrix (**right**) thermal conductivity for in-plane and through-plane directions.

Laminate model: The geometries for a laminate model—both with and without a porous layer between two different plies—are shown in Figure 14. When the plies are

stacked together during the manufacturing process, significant cavities can develop, as shown in Figure 15. The porous layer may have a significantly smaller density and thermal conductivity, thus lowering the overall thermal conductivity of the laminate. The bulk thermal conductivity of the laminate model can be computed similarly to other models. Figure 16 shows example temperature distributions in the two laminate models (with and without a porous layer) as obtained from an analysis performed for computing the through-thickness thermal conductivities of lamina.

For the cases both with and without a porous layer, Figure 17 shows the variation in the laminate thermal conductivity in response to varying the thermal conductivity of a single ply (the thermal conductivities of all the other plies were held constant). As noted from the figure, the porous layer could significantly lower the through-thickness thermal conductivity of the composite.

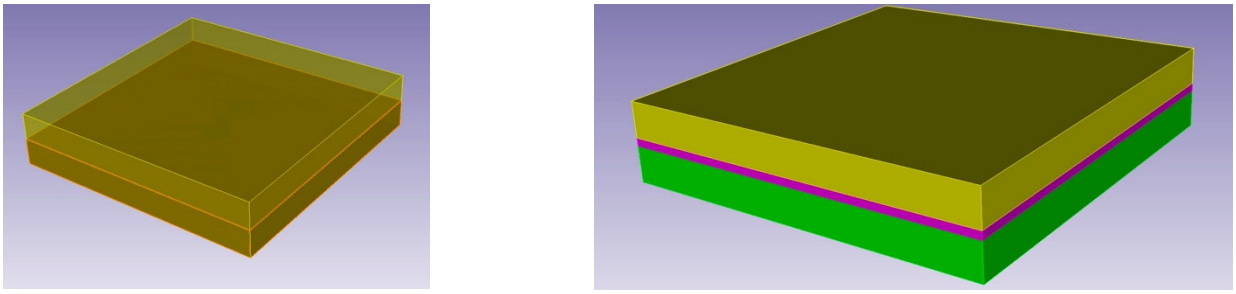

Figure 14. CAD model of a laminate with two plies both with (**left**) and without (**right**) a porous layer between them.

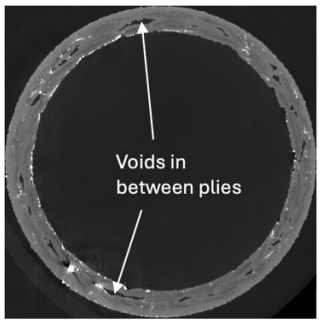

Figure 15. Cross-section of a SiC/SiC cladding tube specimen SETH H [27,28], showing voids between the ply layers.

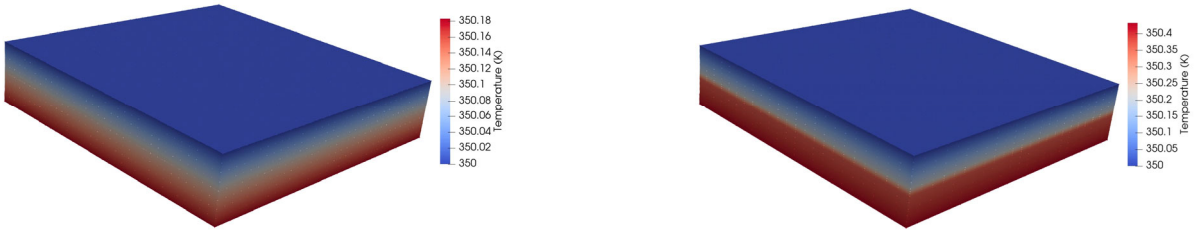

Figure 16. Temperature distributions in the laminate model for the cases without (**left**) and with (**right**) a porous layer between the plies. The porous layer is assumed to have a thermal conductivity of 5 W/m-K and a density of 500 kg/m^3.

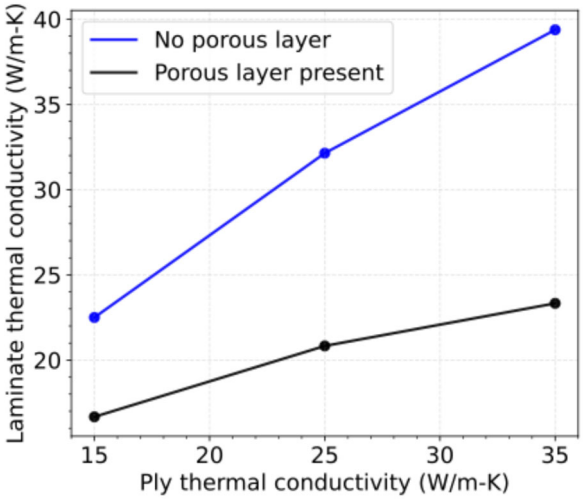

Figure 17. Variation in laminate thermal conductivity in the through-thickness direction when varying the thermal conductivity of a single ply. The thermal conductivity of the other ply was held constant at 45 W/m-K. The porous layer was assumed to have a thermal conductivity of 5 W/m-K, a specific heat capacity of 1000 J/kg-s, and a density of 500 kg/m^3.

4. Conclusions and Future Work

The inherent complexity of composite materials makes it difficult to analyze and optimize their designs. The hierarchical modeling approach presented herein highlights the current status of this ongoing work. This article described and demonstrated a modular approach to modeling composites at different length scales, with a lower length-scale model providing inputs to a higher length-scale model. A matrix model accounted for porosity-caused changes in the matrix thermal properties, and a tow model evaluated the tow thermal conductivity in consideration of the fiber and matrix conductivities and the fiber volume fraction. A ply model evaluated the ply thermal conductivity based on the tow and matrix thermal properties and the specific architecture. Note that porosity in the matrix was indirectly accounted for in the tow and ply models via the matrix thermal conductivity which was calculated in consideration of the porosity in the matrix. A laminate model evaluated the laminate conductivity in consideration of the number of plies, their specific conductivities and orientation, and any possible porosity in-between the ply layers. The evaluated laminate conductivity can be taken as an input to a component model to determine its thermal performance. The SiC composite intended for cladding applications is triaxially braided, with tows along the axial direction and at angles $\pm\theta^\circ$ from the axis. Note that triaxially braided SiC composites have a superior strength-to-weight ratio, improved durability, and enhanced fatigue resistance compared to uniaxially or biaxially reinforced composites. In addition, triaxial braiding allows for composites with relatively more isotropic properties to be manufactured. The angle θ° is around 45 to 60-degrees. In this work, we did not consider triaxial reinforcement in the ply model; instead, we only considered bidirectional tows in mutually orthogonal directions. The advanced architecture of triaxial braiding will be part of future work. Furthermore, porosity due to voids was considered—in simplified fashion—as spherical cavities inside a matrix. Voids in a composite can take arbitrary shapes and feature varying size distributions. Microcracks were often present in the matrix. Such geometries and size distributions of voids and defects could lead to additional anisotropy in the matrix, at least in the local region. The effects of such voids on the thermal performance of SiC/SiC will be explored in future work.

The fibers were considered without interphase material around them; future work will incorporate the interphase. Lastly, the models presented herein will be validated via comparison against the relevant experimental data as the required data become available. For validation purposes, comprehensive data at different length scales will be required.

Currently, the literature offers limited experimental data for such purposes. Future work will entail rigorous validation and improvement in this multiscale modeling approach.

Beyond nuclear applications, silicon carbide fiber-reinforced SiC ceramic matrix composites are promising thermal–structural materials with a broad range of high-end technology applications like friction and wear, electronics, machinery, and chemical industries. Though this work was targeted at the modeling of SiC-SiC fuel cladding for nuclear applications. the multiscale modeling strategy presented herein inherently incorporates inhomogeneous and anisotropic characteristics of a composite material. This physics-informed approach seamlessly bridges the constitutive laws from the matrix modeling at lowest scale to the component modeling at the highest scale. We envision that this multiscale modeling strategy will be highly valuable in designing and predicting innovative composite materials in a variety of applications for specific stress, temperature, and environmental conditions.

Author Contributions: Conceptualization, G.S., J.Y., F.X., T.Y. and P.X.; data curation, F.X. and T.Y.; formal analysis, G.S. and J.Y.; funding acquisition, P.X.; investigation, G.S., J.Y., F.X., T.Y. and P.X.; methodology, G.S. and J.Y.; project administration, P.X.; resources, G.S. and J.Y.; software, G.S.; supervision, P.X.; validation, J.Y., F.X., T.Y. and P.X.; visualization, G.S. and J.Y.; writing—original draft, G.S.; writing—review and editing, G.S., J.Y., F.X., T.Y. and P.X. All authors have read and agreed to the published version of the manuscript.

Funding: This research was funded by U.S. Department of Energy under contract no. DE-AC07-05ID14517. This research made use of the resources of the High-Performance Computing Center at Idaho National Laboratory, which is supported by the Office of Nuclear Energy of the U.S. Department of Energy and the Nuclear Science User Facilities under contract no. DE-AC07-05ID14517.

Data Availability Statement: The data that support the findings of this study are available from the corresponding author upon reasonable request.

Acknowledgments: The U.S. Government retains, and the publisher, by accepting the article for publication, acknowledges that the U.S. Government retains a nonexclusive, paid-up, irrevocable, worldwide license to publish or reproduce the published form of this manuscript or allow others to do so for U.S. Government purposes. The authors also acknowledge the support of DOE Advanced Fuel Campaign on the experimental data collection.

Conflicts of Interest: The authors have no known competing financial interests. This information was prepared as an account of work sponsored by an agency of the U.S. Government. Neither the U.S. Government nor any agency thereof, nor any of their employees, makes any warranty, express or implied, or assumes any legal liability or responsibility for the accuracy, completeness, or usefulness of any information, apparatus, product, or process disclosed, or represents that its use would not infringe privately owned rights. References herein to any specific commercial product, process, or service by trade name, trademark, manufacturer, or otherwise do not necessarily constitute or imply its endorsement, recommendation, or favoring by the U.S. Government or any agency thereof. The views and opinions of the authors expressed herein do not necessarily state or reflect those of the U.S. Government or any agency thereof.

References

1. Katoh, Y.; Snead, L.L.; Henager, C.H., Jr.; Nozawa, T.; Hinoki, T.; Iveković, A.; Novak, S.; De Vicente, S.G. Current status and recent research achievements in SiC/SiC composites. *J. Nucl. Mater.* **2014**, *455*, 387–397. [CrossRef]
2. Carter, C.H., Jr.; Davis, R.F.; Bentley, J. Kinetics and mechanisms of high-temperature creep in silicon carbide: II, chemically vapor deposited. *J. Am. Ceram. Soc.* **1984**, *67*, 732–740. [CrossRef]
3. Katoh, Y.; Nozawa, T.; Snead, L.L.; Ozawa, K.; Tanigawa, H. Stability of SiC and its composites at high neutron fluence. *J. Nucl. Mater.* **2011**, *417*, 400–405. [CrossRef]
4. George, N.M.; Terrani, K.; Powers, J.; Worrall, A.; Maldonado, I. Neutronic analysis of candidate accident-tolerant cladding concepts in pressurized water reactors. *Ann. Nucl. Energy* **2015**, *75*, 703–712. [CrossRef]
5. Delage, J.; Saiz, E.; Al Nasiri, N. Fracture behaviour of SiC/SiC ceramic matrix composite at room temperature. *J. Eur. Ceram. Soc.* **2022**, *42*, 3156–3167. [CrossRef]
6. Hasegawa, A.; Kohyama, A.; Jones, R.H.; Snead, L.L.; Riccardi, B.; Fenici, P. Critical issues and current status of SiC/SiC composites for fusion. *J. Nucl. Mater.* **2000**, *283*, 128–137. [CrossRef]

7. Terrani, K.A.; Pint, B.A.; Parish, C.M.; Silva, C.M.; Snead, L.L.; Katoh, Y. Silicon carbide oxidation in steam up to 2 MPa. *J. Am. Ceram. Soc.* **2014**, *97*, 2331–2352. [CrossRef]
8. Avincola, V.A.; Grosse, M.; Stegmaier, U.; Steinbrueck, M.; Seifert, H.J. Oxidation at high temperatures in steam atmosphere and quench of silicon carbide composites for nuclear application. *Nucl. Eng. Des.* **2015**, *295*, 468–478. [CrossRef]
9. Katoh, Y.; Ozawa, K.; Shih, C.; Nozawa, T.; Shinavski, R.J.; Hasegawa, A.; Snead, L.L. Continuous SiC fiber, CVI SiC matrix composites for nuclear applications: Properties and irradiation effects. *J. Nucl. Mater.* **2014**, *448*, 448–476. [CrossRef]
10. Koyanagi, T.; Katoh, Y.; Singh, G.; Snead, M. SiC/SiC cladding materials properties handbook. In *Nuclear Technology Research and Development*; U.S. Department of Energy: Washington, DC, USA, 2017.
11. Carpenter, D.M. An Assessment of Silicon Carbide as a Cladding Material for Light Water Reactors. Doctoral Dissertation, Massachusetts Institute of Technology, Cambridge, MA, USA, 2010.
12. Koyanagi, T.; Kato, Y. *Systematic Technology Evaluation Program for SiC-Based BWR Channel Box (No. ORNL/SPR-2019/1120)*; Oak Ridge National Laboratory (ORNL): Oak Ridge, TN, USA, 2019.
13. Kohyama, A.; Hinoki, T.; Mizuno, T.; Kunugi, T.; Sato, M.; Katoh, Y.; Park, J.S. R & D of advanced material systems for reactor core component of gas cooled fast reactor. In Proceedings of the American Nuclear Society-International Congress on Advances in Nuclear Power Plants 2005, ICAPP'05, Seoul, Republic of Korea, 15–19 May 2005.
14. Charpentier, L.; Dawi, K.; Balat-Pichelin, M.; Bêche, E.; Audubert, F. Chemical degradation of SiC/SiC composite for the cladding of gas-cooled fast reactor in case of severe accident scenarios. *Corros. Sci.* **2012**, *59*, 127–135. [CrossRef]
15. Forsberg, C.W.; Peterson, P.F.; Kochendarfer, R.A. Design options for the advanced high-temperature reactor. In Proceedings of the ICAPP'08, Anaheim, CA, USA, 8–12 June 2008; Volume 8, pp. 8–12.
16. Braun, J.; Sauder, C.; Rouillard, F.; Balbaud-Célérier, F. Mechanical behavior of SiC/SiC composites after exposure in high temperature liquid sodium for Sodium Fast Reactors applications. *J. Nucl. Mater.* **2021**, *546*, 152743. [CrossRef]
17. Katoh, Y.; Snead, L.L.; Henager, C.H., Jr.; Hasegawa, A.; Kohyama, A.; Riccardi, B.; Hegeman, H. Current status and critical issues for development of SiC composites for fusion applications. *J. Nucl. Mater.* **2007**, *367*, 659–671. [CrossRef]
18. Stone, J.G.; Schleicher, R.; Deck, C.P.; Jacobsen, G.M.; Khalifa, H.E.; Back, C.A. Stress analysis and probabilistic assessment of multi-layer SiC-based accident tolerant nuclear fuel cladding. *J. Nucl. Mater.* **2015**, *466*, 682–697. [CrossRef]
19. Singh, G.; Sweet, R.; Brown, N.R.; Wirth, B.D.; Katoh, Y.; Terrani, K. Parametric evaluation of SiC/SiC composite cladding with UO_2 fuel for LWR applications: Fuel rod interactions and impact of nonuniform power profile in fuel rod. *J. Nucl. Mater.* **2018**, *499*, 155–167. [CrossRef]
20. Singh, G.; Terrani, K.; Katoh, Y. Thermo-mechanical assessment of full SiC/SiC composite cladding for LWR applications with sensitivity analysis. *J. Nucl. Mater.* **2018**, *499*, 126–143. [CrossRef]
21. Ben-Belgacem, M.; Richet, V.; Terrani, K.A.; Katoh, Y.; Snead, L.L. Thermo-mechanical analysis of LWR SiC/SiC composite cladding. *J. Nucl. Mater.* **2014**, *447*, 125–142. [CrossRef]
22. Li, W.; Shirvan, K. Finite element analysis of the SiC/SiC composite clad deformation in the presence of spacer grids. *Ann. Nucl. Energy* **2020**, *137*, 107114. [CrossRef]
23. Li, W.; Shirvan, K. ABAQUS analysis of the SiC cladding fuel rod behavior under PWR normal operation conditions. *J. Nucl. Mater.* **2019**, *515*, 14–27. [CrossRef]
24. Alabdullah, M.; Ghoniem, N.M. Damage mechanics modeling of the non-linear behavior of SiC/SiC ceramic matrix composite fuel cladding. *J. Nucl. Mater.* **2019**, *524*, 296–311. [CrossRef]
25. Blacker, T.D.; Owen, S.J.; Staten, M.L.; Quadros, W.R.; Hanks, B.; Clark, B.W.; Meyers, R.J.; Ernst, C.; Merkley, K.; Morris, R.; et al. *CUBIT Geometry and Mesh Generation Toolkit 15.1 User Documentation (No. SAND-2016-1649R)*; Sandia National Laboratory (SNL-NM): Albuquerque, NM, USA, 2016.
26. Permann, C.J.; Gaston, D.R.; Andrš, D.; Carlsen, R.W.; Kong, F.; Lindsay, A.D.; Miller, J.M.; Peterson, J.W.; Slaughter, A.E.; Stogner, R.H.; et al. MOOSE: Enabling massively parallel multiphysics simulation. *SoftwareX* **2020**, *11*, 100430. [CrossRef]
27. Xu, F.; Yao, T.; Xu, P.; Schulthess, J.L.; Matos, M.D.; Gonderman, S.; Gazza, J.; Kane, J.J.; Cordes, N.L. Multi-Scale Characterization of Porosity and Cracks in Silicon Carbide Cladding after Transient Reactor Test Facility Irradiation. *Energies* **2023**, *17*, 197. [CrossRef]
28. Schulthess, J.; Kamerman, D.; Winston, A.; Pomo, A.; Trowbridge, T.; Pu, X.; Woolstenhulme, N.; Imholte, D.; Jensen, C.; Wachs, D. Post-transient examination of performance of uranium silicide fuel and silicon-carbide composite cladding under reactivity-initiated accident conditions. *J. Nucl. Mater.* **2022**, *560*, 153520. [CrossRef]